Characterization of Iodovinylmisonidazole as a Marker for Myocardial Hypoxia

Gary V. Martin, Joseph E. Biskupiak, James H. Caldwell, Janet S. Rasey and Kenneth A. Krohn

Division of Cardiology, Seattle Veterans Affairs Medical Center and Departments of Radiology and Radiation Oncology, University of Washington, Seattle, Washington

Misonidazole and related compounds are metabolically trapped in viable cells as a function of reduced cellular pO_2. [^{18}F]fluoromisonidazole has been used to detect hypoxia in the heart and in tumors noninvasively with positron emission tomography. The purpose of this study was to characterize the uptake of the iodinated misonidazole congener iodovinylmisonidazole (IVM) in ischemic myocardium. In six open chest dogs (Group 1), the left anterior descending (LAD) coronary artery was partially occluded and in four dogs (Group 2), demand ischemia was produced by the combination of atrial pacing and catecholamine infusion in the presence of a LAD stenosis. [^{131}I]IVM (5–15 μCi/kg, i.v.) was given following the onset of ischemia. Tracer deposition was measured by postmortem tissue sampling 4 hr postinjection and compared to microsphere myocardial blood flow (MBF) measurements made at baseline and at 2 hr postinjection. In Group 1, regional IVM deposition in heart samples within the ischemic area was inversely related to MBF with maximum tissue:blood ratios of 3.2. For a given level of reduced blood flow, IVM uptake was higher in the subendocardium indicating a greater vulnerability of the subendocardium to reductions in oxygen delivery. In Group 2, enhanced IVM deposition was detected as a result of demand ischemia, even in some regions where absolute flow was normal or increased from baseline, indicating that flow per se is not the principal determinant of tracer uptake. We conclude that IVM is a promising marker for myocardial hypoxia with potential clinical application using gamma camera imaging.

J Nucl Med 1993; 34:918–924

Misonidazole and related compounds are metabolically trapped in viable cells as a function of reduced cellular pO_2. Hypoxia-dependent binding of these drugs has been shown in a variety of tissues in vitro and in vivo (1–7). Fluorine-18-labeled fluoromisonidazole has been used with positron emission tomography (PET) to image hypoxic tissues in the heart (8,9) and in tumors (10), and preliminary human studies have shown promise (11,12). In the heart,

an important potential application is the detection of chronically hypoxic but viable myocardium, which could be targeted for revascularization.

We have recently described the synthesis of an iodinated analogue of misonidazole (IVM, (E)-5-(2-nitroimidazolyl)-4-hydroxy-1-iodopent-1-ene,3) (13). An iodinated hypoxia tracer provides the possibility of imaging hypoxic tissues using a gamma camera, a less expensive and more widely available imaging modality than PET. Preliminary in vitro studies have suggested that the oxygen sensitivity of binding for IVM is similar to that of fluoromisonidazole (13). However, the biodistribution characteristics of this molecule have not been defined. The goals of this study were to characterize the binding of IVM in ischemic myocardium in vivo and to compare its deposition to myocardial flow measured with radiolabeled microspheres.

METHODS

Iodine-131-IVM Radiolabeling

Iodine-131-labeled IVM was prepared as described previously (13). To the commercial solution of [^{131}I]NaI in 0.1N NaOH (0.010 ml, 6.62 mCi, specific activity 1280 Ci/mmol) were successively added (E)-5-(2-nitroimidazolyl)-4-hydroxy-1-tributylstannylpent-1-ene (0.2 mg, 0.042 mmol) in THF (0.1 ml) and NaOAc buffer (0.61 M, pH 4.5, 0.1 ml). The resultant stirred mixture was treated with a solution of H_2O_2 (30% aq)/HOAc (2:1)(0.025 ml) within the sealed vial. After 30 min, the reaction was quenched by the addition of 5% aq $Na_2S_2O_3$ solution (0.1 ml). The entire crude reaction mixture (0.335 ml) was loaded onto a Whatman ODS-3 reverse phase column, followed by elution with 1:1 EtOH-water. Iodine-131-IVM (3.82 mCi, 58% radiochemical yield) was isolated after 11 min, in approximately 4 ml of solution. Postpurification analysis of the isolated solution by TLC (silica gel, 2:3 CH_3CN/$CHCl_3$, R_f0.41) and HPLC revealed identical chromatographic characteristics to that of unlabeled IVM. The specific activity of the isolated material was determined (UV absorbance @ 280 nm, ε 3230) to be 450 Ci/mmol. The radiochemical purity of the sample was >98.5%.

Animal Preparation and Surgery

Ten mongrel dogs (25–34 kg) were sedated with intravenous thiamyl sodium (20 mg/kg) and intubated. General anesthesia was maintained by mechanically ventilating the animals with Halothane and oxygen. Arterial blood gases were intermittently monitored and ventilatory parameters were adjusted to maintain phys-

iological blood pH. Arterial pO_2 in each animal was greater than 160 mmHg. A left thoracotomy was performed, the pericardium opened and a variable hydraulic occluder placed loosely around the left anterior descending (LAD) coronary artery. Additional catheters were placed in the left atrium, the left carotid artery and internal jugular vein and a peripheral foreleg vein. The electrocardiogram (ECG) and arterial blood pressure were continuously monitored. In each animal, a doppler wall thickening crystal (14) was sewn to the epicardial surface within the LAD distribution to monitor regional wall thickening. In four animals, a crystal was placed in the circumflex coronary distribution to measure wall thickening in the normally perfused region. Systolic wall thickening was defined as the absolute change in wall thickness occurring between the ECG R-wave and the dichrotic notch of the aortic pressure trace. In four animals, pacing wires were sutured to the left atrial appendage.

Experimental Protocols

Two groups of animals were studied. In Group 1 (n = 6), partial occlusion of the LAD was accomplished by slowly tightening the variable occluder while constantly monitoring the regional wall thickening signal until wall thickening was noticeably decreased but not abolished. This stenosis was maintained until just prior to sacrifice, when the occluder was loosened to allow reperfusion for several minutes to assess the effects of reperfusion on wall motion. Each animal received prophylactic lidocaine (2 mg/kg i.v. bolus followed by a constant infusion of 1 mg/min) to minimize the likelihood of ventricular fibrillation. Immediately following the onset of ischemia [^{131}I]IVM (5–15 μCi/kg) was administered as an intravenous bolus. The injected product was synthesized as described previously (13) and was >98.5% radiochemically pure as determined by thin layer chromatography. Serial blood samples were taken throughout the study to determine the rate of blood clearance. Microsphere myocardial blood flow (MBF) measurements were made at baseline (prior to the stenosis and IVM injection) and at 2 hr post-IVM injection using the reference organ technique (15). Three to five million radiolabeled ([57]Co, [85]Sr) 15-micron spheres (Du Pont New England Nuclear), were injected into the left atrium while a reference organ sample was drawn from the carotid catheter at 15 ml/min for 1 min. At 4 hr, the animals were euthanized using a lethal intravenous dose of potassium chloride.

In a separate series of experiments, Group 2 (n = 4), we studied myocardial IVM deposition during demand ischemia. For these experiments, a less severe stenosis was used that did not produce measurable changes in either wall thickening or the ECG. To achieve this stenosis the occluder was slowly tightened while the ECG and wall motion signals were continuously monitored, until mild decreases in wall motion were observed. The occluder was then loosened slightly until wall motion normalized. After the stenosis was applied, pacing tachycardia and a catecholamine infusion (epinephrine 0.001 μg/ml, norepinephrine 0.004 μg/ml) were initiated and titrated to achieve a twofold to threefold increase in the rate-pressure product (heart rate × systolic blood pressure). IVM was administered and microsphere flow measurements were made as in Group 1.

Tissue Sampling

Postmortem, the heart was rapidly removed, rinsed of excess blood and cut into four slices, perpendicular to the long-axis of the left ventricle. The two outer slices were incubated in nitroblue tetrazolium (NBT) to identify areas of infarction. The two center slices were sectioned into 16 radial segments per slice, which were

further cut into three transmural pieces for a total of 96 pieces (370 ± 160 mg) per heart. Each piece was weighed and counted for ^{131}I activity in a 3" NaI well counter. To minimize cross-talk with the ^{131}I, the samples were recounted for microsphere activity several days later. Additional samples (n = 5) of brain, liver, kidney, skeletal muscle, small intestine, lung, fat and thyroid were also taken from Group 1 dogs for gamma well counting. The myocardial well count data were corrected for piece weight and expressed as a tissue-to-blood ratio using the blood counts taken just prior to sacrifice at 4 hr.

In this study, the MBF data in each piece are expressed as the ratio of the flow during ischemia to baseline flow, for the following reasons. Given the very broad range of flows (fivefold or greater depending on piece size) in normal myocardium (16), absolute flow measurements in a given tissue sample at a single time point can be quite ambiguous with respect to the presence or absence of ischemia. For example, some samples normally have flows which are 50% of the mean flow for the entire myocardium. However, if it can be shown that flow in a given sample has fallen to 50% of its baseline in response to an intervention, the presence of ischemia is more assured. A second general problem with the use of absolute flows when presenting mean data is interanimal variability with respect to anesthesia and hemodynamics.

Statistical Analysis

Group data are reported throughout as mean ± the s.d. Differences in group means for the analysis of IVM deposition as function of transmural location were evaluated using a paired t-test. Differences in group means for the analysis of the IVM biodistribution data were evaluated using the Wilcoxon signed-rank test. Differences were considered significant when $p < 0.05$.

RESULTS

Hemodynamics

The hemodynamic data are shown in Table 1. The administration of IVM caused no noticeable hemodynamic changes in any of the animals. In Group 1 dogs, partial stenosis of the LAD was associated with only minimal changes in systemic hemodynamics. Heart rate and blood pressure both trended downward during the 4-hour protocol, effects most likely attributable to increasing depth of anesthesia. Regional wall thickening was significantly reduced to an average of 34% ± 14% of baseline during the ischemic period and improved significantly to 51% ± 19% following reperfusion at the end of the study. In the dogs with demand ischemia (Group 2), the heart rate and blood pressure were significantly elevated as a result of the catecholamine infusion and atrial pacing. The double product (heart rate × systolic blood pressure) was increased by 248% ± 57% over baseline. Wall thickening fell to a mean of 69% ± 36% of baseline in the ischemic region and increased to a mean of 112% ± 4% of baseline in the nonischemic region of the ventricle. There was an absence of infarction in each heart by NBT staining.

Blood Clearance and Organ Biodistribution

A representative blood clearance curve for IVM is shown in Figure 1. Blood clearance exhibited a biphasic pattern with an initial rapid distribution phase followed by a more gradual clearance phase. The mean $T_{1/2}$ of the clear-

Group 1, n = 6			
Time (min)	Heart rate (min⁻¹)	Mean AP (mmHg)	LAD WTh. (%baseline)
0 (Baseline)	105 ± 16	86 ± 11	100
30	100 ± 13	81 ± 15	53 ± 23
60	99 ± 13	82 ± 17	43 ± 15
120	95 ± 15	77 ± 11	37 ± 15
180	91 ± 16	77 ± 13	33 ± 14
240	92 ± 21	77 ± 16	32 ± 17
Mean ischemia	95 ± 15	78 ± 16*	34 ± 14*
Reperfusion	89 ± 19	71 ± 14*	51 ± 19*†

Group 2, n = 4				
Time (min⁻¹)	Heart rate (min⁻¹)	Mean AP (mmHg)	LAD WTh. (%baseline)	Circ. WTh. (%baseline)
0 (Baseline)	98 ± 26	78 ± 25	100	100
30	160 ± 16	111 ± 18	81 ± 30	120 ± 9
60	158 ± 27	108 ± 8	78 ± 36	118 ± 7
120	164 ± 15	112 ± 6	63 ± 32	109 ± 1
180	168 ± 35	111 ± 4	66 ± 35	104 ± 5
240	169 ± 37	107 ± 3	49 ± 27	105 ± 6
Mean ischemia	163 ± 15*	112 ± 5*	69 ± 36*	112 ± 4*

*$p < 0.05$ versus baseline.
†$p < 0.05$ versus ischemia.

Data are mean ± s.d. Mean AP = mean arterial pressure. WTh = systolic wall thickening expressed as a percentage of baseline in the region of the myocardium supplied by the left anterior descending (LAD) and circumflex (Circ.) coronary arteries. Mean ischemia = mean of all measurements taken during the ischemic period. Reperfusion = measurements taken several minutes after the 240-min recording, during reperfusion. Microsphere blood flow measurements were made at the 0- and 120-min time points.

ance phase was 4.6 ± 0.3 hr. The apparent volume of distribution for IVM was 0.7 + 0.1 l/kg, consistent with distribution into the total-body water space. The biodistribution data are shown in Table 2. The content of IVM in blood at 4 hr postinjection averaged 0.0029% ± 0.0012% of the injected dose per gram. Relative to blood, the IVM content was significantly higher in liver and kidney with

FIGURE 1. Representative arterial blood clearance following an intravenous injection of [¹³¹I]IVM from a single study. Clearance is biphasic with an initial rapid distribution phase followed by a slower clearance phase.

tissue-to-blood ratios of 3.1 ± 0.5 and 1.9 ± 0.4, respectively. The tissue-to-blood ratios for lung, thyroid and small intestine were also consistently in excess of one. IVM deposition in normal heart, brain, skeletal muscle and fat was similar to blood at 4 hr.

Myocardial IVM Deposition

The relationship between IVM deposition and myocardial blood flow from a representative Group 1 study is shown in Figure 2. Relatively uniform IVM deposition was present in samples where flow was greater than about 70% of baseline. Among samples with flows less than 70% of baseline, there was a generally inverse relationship between flow and IVM deposition. Figure 3 shows the composite data for all Group 1 dogs comprising a total of 576 heart samples. The IVM data are expressed as the tissue: blood ratio using the blood counts taken at 4 hr. The MBF data are expressed as the ratio of the poststenosis to baseline flow. In nonischemic areas, IVM deposition is quite uniform despite the broad range of normal flows. In samples taken from outside the anatomically defined nonischemic regions, IVM deposition and flow were inversely related with a maximum normalized IVM tissue to blood ratio of 3.2. This relationship is qualitatively similar to that which has been observed with fluoromisonidazole under similar experimental conditions (7), although the maximum
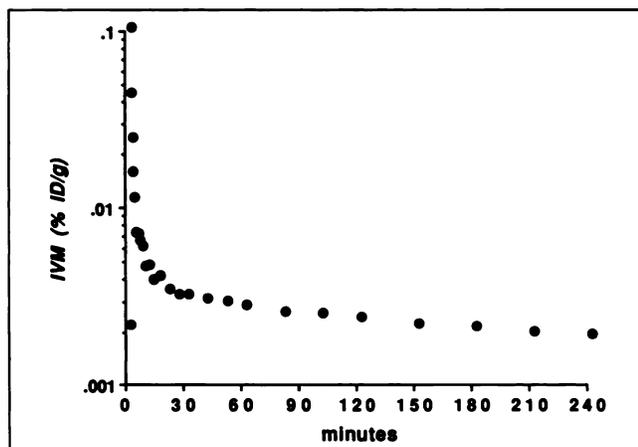
TABLE 2
IVM Biodistribution Data at 4 Hours Postinjection

Organ	%ID/g	Tissue-to-blood ratio
Blood	.0029 ± .0012	1.0
Heart (normal)	.0033 ± .0017	1.1 ± 0.2
Lung	.0047 ± .0025	1.6 ± 0.3*
Brain	.0034 ± .0017	1.2 ± 0.2
Thyroid	.0038 ± .0017	1.3 ± 0.2*
Skeletal muscle	.0029 ± .0010	1.0 ± 0.2
Small intestine	.0048 ± .0020	1.4 ± 0.3*
Fat	.0025 ± .0010	0.9 ± 0.2
Liver	.0091 ± .0042	3.1 ± 0.5*
Kidney	.0063 ± .0029	1.9 ± 0.4*

*p < 0.05 vs. blood.
Data are mean ± s.d., n = 6 studies.

normalized values are slightly lower for IVM than for fluoromisonidazole.

It can also be observed that for a given severity of ischemia, as defined by flow, there is a fairly broad range of IVM depositions. To determine whether some of the heterogeneity in IVM binding might relate to transmural location, the same data from Group 1 dogs were grouped on the basis of the ischemic to baseline flow ratio into 3 subgroups; samples with a flow ratio of less than 0.4 (severe ischemia), samples with a flow ratio between 0.4 and 0.8 (mild ischemia), and samples with a flow ratio of greater than 0.8 (no ischemia). Samples in each group were further categorized based on their transmural location as epicardium, midwall or endocardium. The results of this analysis are shown in Figure 4 and indicate that for a given flow, IVM deposition was highest in the endocardium and lowest
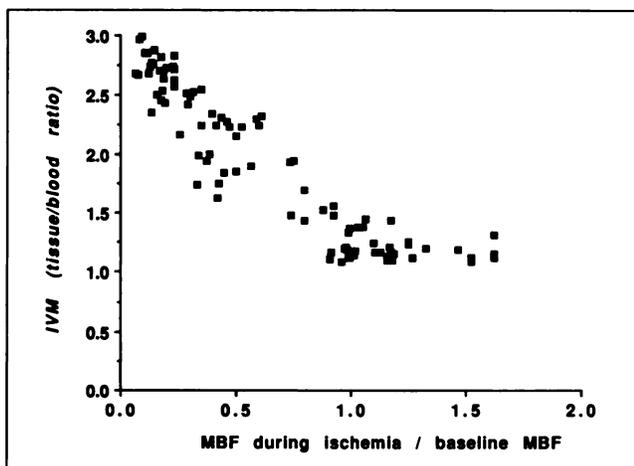

FIGURE 3. Tissue sampling data (n = 576 samples) from all Group 1 experiments in which regional ischemia was produced by partial stenosis of the LAD coronary artery showing the relationship between regional myocardial blood flow and IVM uptake. The IVM data are expressed as a tissue-to-blood ratio using the blood counts taken at 4 hr just prior to death. The microsphere blood flow data are expressed as the ratio of the flow following th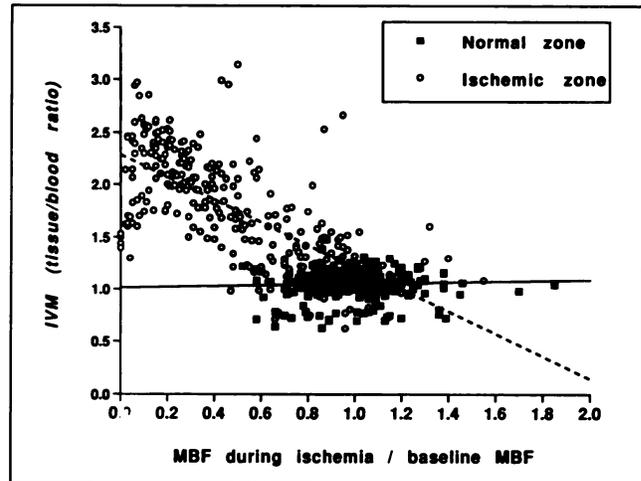e application of the LAD stenosis to the baseline flow. The tissue samples from the center of the nonischemic zone are shown as closed circles and all remaining samples as open squares. Curve fits determined using the linear least-squares method are also shown separately for the ischemic (dashed line) and nonischemic (solid line) tissue samples. In nonischemic myocardium, IVM deposition is quite uniform despite the broad range of flows (regression equation y = 1.08 + 0.002x, r = 0.05). In ischemic tissue, IVM deposition is inversely related to flow (regression equation y = 2.3 − 1.07x, r = 0.70).

in the epicardium. Also shown in Figure 4 are the mean absolute flows for each flow ratio category. It is noteworthy that for a given flow ratio, greater IVM deposition occurred in the subendocardium despite greater absolute flows.
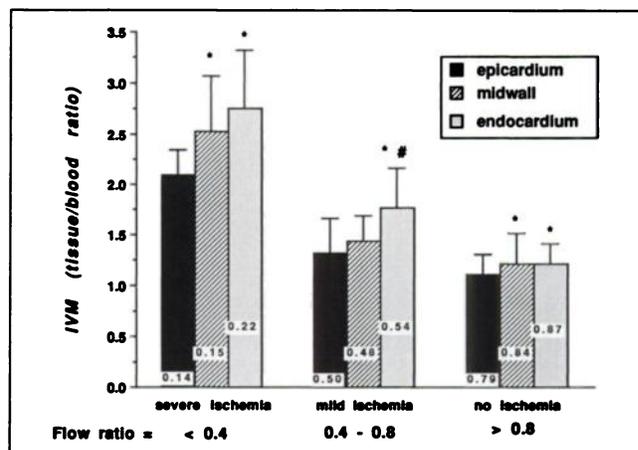

FIGURE 2. Tissue sampling data (n = 96 samples) from a single experiment in which regional ischemia was produced by partial stenosis of the left anterior descending (LAD) coronary artery showing the relationship between regional myocardial blood flow and IVM uptake. The IVM data are expressed as a tissue-to-blood ratio using the blood counts taken at 4 hr just prior to death. The microsphere blood flow data are expressed as the ratio of the flow following the application of the LAD stenosis to the baseline flow.

FIGURE 4. Tissue sampling data (n = 576 samples) from all Group 1 experiments showing the relationship between transmural location and IVM uptake. For this analysis, each tissue sample was categorized on the basis of flow (the ratio of the flow following the application of the LAD stenosis to the baseline flow) and transmural location. The mean absolute flows for each category are shown within the bars. With either mild or severe ischemia, IVM uptake is higher in the subendocardium than in the subepicardium. *p < 0.05 versus epicardium; #p < 0.05 vs. midwall.
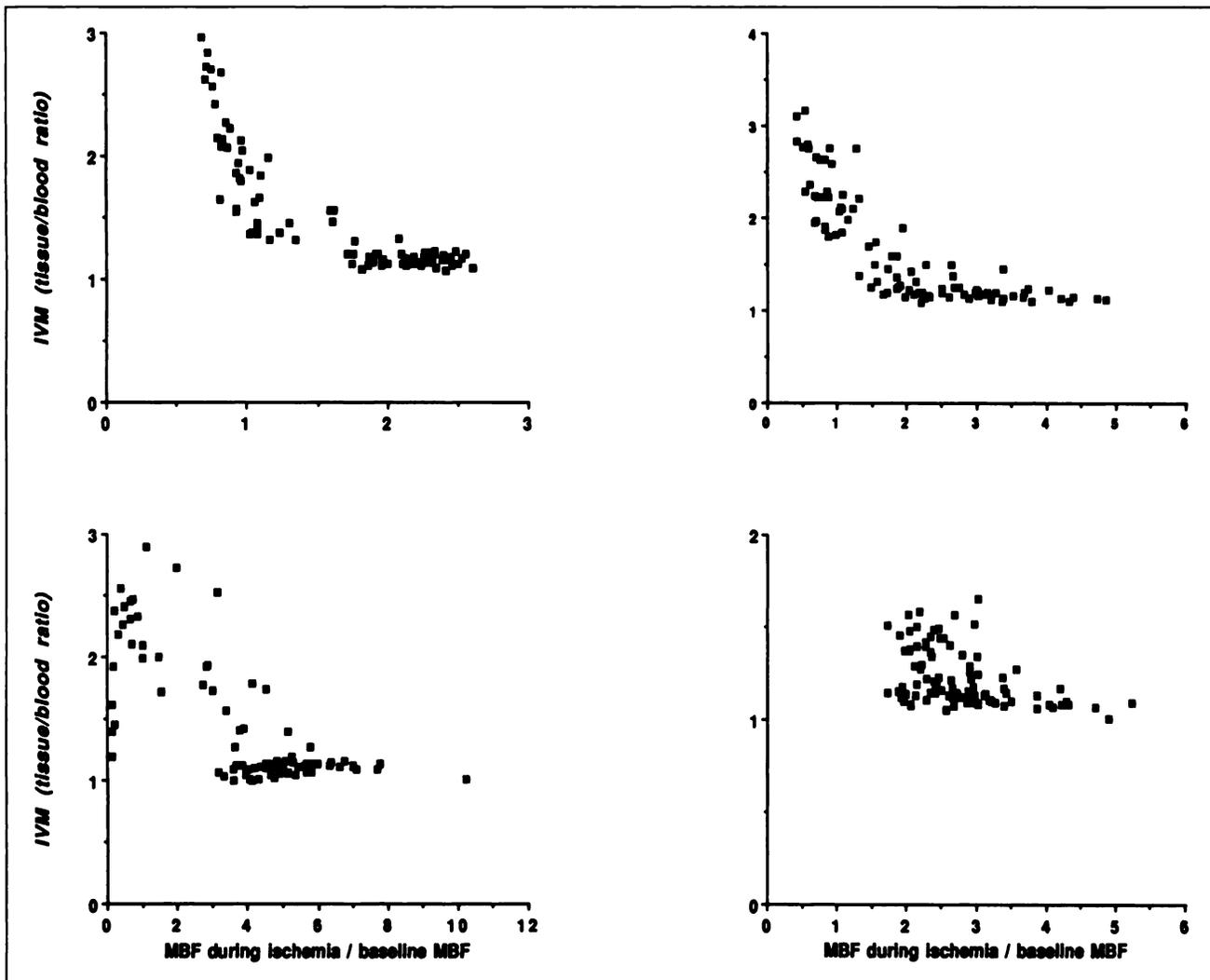
FIGURE 5. Tissue sampling data from the individual Group 2 experiments in which regional ischemia was produced by catecholamine and pacing stimulation in the setting of a partial stenosis of the LAD coronary artery. Shown is the relationship between regional myocardial blood flow and IVM uptake for the 96 samples from each study.

Figure 5 shows the data from the individual Group 2 studies in which ischemia was produced by increased myocardial work in the presence of a partial coronary stenosis. The relationship between flow and IVM deposition in these experiments was qualitatively similar to that of the Group 1 studies. However, it is notable that enhanced IVM deposition was observed in some tissue samples in which flow was more than double the baseline flow.

DISCUSSION

The biodistribution characteristics and myocardial uptake of an iodinated hypoxia tracer, IVM, were determined in open-chest dogs subjected to regional myocardial ischemia. Ischemia was produced by either restricting resting myocardial blood flow or by catecholamine and pacing stimulation in the setting of a coronary stenosis, which did not effect resting flow but also did not allow flow to increase in proportion to metabolism. In each animal, the tissue retention of IVM was enhanced in regions of absolute or relative underperfusion, indicating that [^{123}I]IVM

may be useful for detecting hypoxic tissues using a gamma camera.

The biodistribution data show that IVM concentrations at 4 hr postinjection are highest in liver and kidney. The reason for enhanced hepatic and renal deposition is unknown but likely relates to metabolism of the drug in the liver and urinary excretion. The avid liver uptake could conceivably pose problems for imaging the heart, especially the inferior wall. This potential problem might be minimized by using SPECT, as opposed to planar imaging. However, an assessment of the utility of this molecule as an imaging agent awaits further testing. Uptake in thyroid was only slightly in excess of blood, possibly reflecting the small amount of free iodide (less than 0.2% of the total) in the injectate. This suggests that any deiodination which could have occurred in vivo was quantitatively unimportant, as much higher levels in the thyroid would be expected. The reason for enhanced lung uptake is not known. However, since the reported uptake is per gram, this should not be a problem for cardiac imaging given the

much lower density of the lungs. The plasma clearance $T_{1/2}$ (4.6 hr) is similar to that reported for fluoromisonidazole (7). The relatively slow clearance of IVM from the blood suggests that hypoxic myocardium would be best visualized on images obtained late (2–4 hr) after injection, as has been reported for [^{18}F]fluoromisonidazole.

The two protocols used in these studies were designed to study tissue hypoxia of mild to moderate severity. In none of the hearts was necrosis detected by histochemical (NBT) staining. In the Group 1 animals, systolic wall thickening in the ischemic region was depressed but not abolished and showed partial recovery during brief reperfusion, evidence for functional viability. In Group 2, demand ischemia resulted in only mild wall motion abnormalities. Thus, IVM binding can occur at levels of tissue hypoxia which are sufficient to cause abnormalities in wall motion, but not so severe as to cause significant tissue necrosis. This compound might therefore be useful clinically in the identification of patients with chronically underperfused but viable (hibernating) myocardium.

The current data demonstrate that hypoxia tracers provide information which is different from that provided by flow tracers. In nonischemic myocardium, there is normally a broad range of regional flows, yet a rather uniform retention of IVM, even in tissue samples where flow is half the mean. When flow is restricted pathologically, tissue pO_2 falls, as reflected by enhanced IVM retention, and there is a general inverse relationship between flow and IVM. However, there is not a precise relationship between IVM and flow, as illustrated by the heterogeneity of IVM deposition at a given level of reduced flow. The lack of a precise relationship between IVM deposition and flow most likely reflects that while flow is an important indicator of oxygen delivery, hypoxia tracers reflect the balance between oxygen delivery and utilization. The catecholamine/pacing experiments demonstrate that similar degrees of tissue hypoxia may occur over a broad range of absolute flows, depending on the metabolic demands.

One limitation of the current study is that the IVM data reflect the integral of IVM binding over the entire 4-hr ischemic period, while the microsphere blood flow data are "snapshots" taken at a single time point during the 4-hr period. Therefore, an important question is whether the single flow measurement is a quantitatively realistic reflection of the mean or integrated blood flow throughout the 4-hr period. The hemodynamic stability of our animal model over the 4-hr ischemic period suggests that major changes in myocardial blood flow did not occur. In nonischemic myocardium, temporal heterogeneities in MBF are small compared to spatial heterogeneities (16), but we are unaware of published data regarding the temporal stability of MBF during prolonged moderate ischemia. Thus, the lack of a true measure of mean MBF during the 4-hr protocol remains a possible contributing explanation for the lack of a more precise relationship between flow and IVM uptake in the current study.

The current data also provide evidence that for a given

level of reduced flow, tissue hypoxia is more severe in the subendocardium than in the subepicardium. While it has been postulated that the subendocardium exhibits a greater metabolic susceptibility to ischemia than does the subepicardium, there is little direct experimental evidence. The current data are consistent with those of Murray et al. (17) who reported that for a given level of flow reduction, myocardial ATP levels fall more rapidly in the endocardium than in the epicardium. Lowe and colleagues (18) also reported that under conditions of severe ischemia, and where transmural flow is uniformly depressed, myocardial necrosis starts first in the subendocardium. These data are consistent with the concept that the metabolic consequences of ischemia reflect not only the severity of underperfusion, but the spatial (transmural) location, and therefore that the severity of the metabolic insult cannot be defined by measurements of flow (either relative or absolute). Hypoxia tracers such as IVM may therefore have an important role in the evaluation of patients with ischemic heart disease, providing information not obtainable by flow tracers alone. The current study suggests the possibility of using [^{123}I]IVM to noninvasively assess myocardial oxygen status.

ACKNOWLEDGMENTS

REFERENCES

1. Chapman JD, Baer K, Lee J. Characteristics of the metabolism-induced binding of misonidazole to hypoxic mammalian cells. *Cancer Res* 1983;43: 1523–1528.
2. Hoffman JM, Rasey JS, Spence A, Shaw D, Krohn K. Binding of the hypoxia tracer [3H]misonidazole in cerebral ischemia. *Stroke* 1987;18:168–176.
3. Koch CJ, Stobbe CC, Baer KA. Metabolism induced binding of C-14 misonidazole to hypoxic cells: kinetic dependance on oxygen concentration and misonidazole concentration. *Int J Radiat Oncol Biol Phys* 1984;10:1327–1332.
4. Rasey JS, Grunbaum Z, Magee S, et al. Characterization of radiolabeled fluoromisonidazole as a probe for hypoxic cells. *Radiat Res* 1987;111:292–304.
5. Martin GV, Cerqueira MD, Caldwell JH, Rasey JS, Embree L, Krohn KA. Fluoromisonidazole: a metabolic marker of myocyte hypoxia. *Circ Res* 1990;67:240–244.
6. Shelton ME, Dence CS, Hwang DR, Welch MJ, Bergmann SR. Myocardial kinetics of fluorine-18 misonidazole: a marker of hypoxic myocardium. *J Nucl Med* 1989;30:351–358.
7. Martin GV, Rasey JS, Caldwell JC, Grunbaum Z, Krohn KA. Fluoromisonidazole uptake in ischemic canine myocardium. *J Nucl Med* 1989;30: 194–201.
8. Shelton ME, Dence CS, Hwang D-R, Herrero P, Welch MJ, Bergmann SR. In vivo delineation of myocardial hypoxia during coronary occlusion using fluorine-18 fluoromisonidazole and positron emission tomography: a potential approach for identification of jeopardized myocardium. *J Am Coll Cardiol* 1990;16:477–485.
9. Martin GV, Caldwell JH, Graham MM, et al. Noninvasive detection of hypoxic myocardium using 18-F-fluoromisonidazole and positron emission tomography. *J Nucl Med* 1992;33:2202–2208.
10. Rasey JS, Koh W-J, Grierson JR, Grunbaum Z, Krohn KA. Radiolabeled fluoromisonidazole as an imaging agent for tumor hypoxia. *Int J Radiat Oncol Biol Phys* 1989;17:985–992.
11. Revenaugh JR, Caldwell JH, Martin GV, Grierson JL, Krohn KA. Positron emission tomography (PET) imaging of myocardial hypoxia with 18F-fluoromisonidazole (FMISO) in post myocardial infarction patients [Abstract]. *Circulation* 1991;84:II-424.

12. Koh W-J, Rasey JS, Evans ML, et al. Imaging of hypoxia in human tumors with [F18]-fluoromisonidazole. *Int J Radiat Oncol Biol Phys* 1991;22:199–212.

13. Biskupiak JE, Grierson JR, Rasey JS, Martin GV, Krohn KA. Synthesis of an (iodovinyl)misonidazole derivative for hypoxia imaging. *J Med Chem* 1991;34:2165–2168.

14. Hartley CJ, Latson LA, Michael LH, Seidel CL, Lewis RM, Entman ML. Doppler measurement of myocardial thickening with a single epicardial transducer. *Am J Physiol* 1983;251:H1044–H1055.

15. Heymann MA, Payne DB, Hoffman JIE, Rudolph AM. Blood flow mea-surements with radionuclide-labelled particles. *Prog Cardiovasc Dis* 1977; 20:55–79.

16. King RB, Bassingthwaighte JB, Hales JRS, Powell LB. Stability of heter-ogeneity of myocardial blood flow in normal awake baboons. *Circ Res* 1985;57:285–295.

17. Murray CE, Reimer KA, Hill ML, Yamasawa I, Jennings RB. Collateral blood flow and transmural location: independent determinants of ATP in ischemic canine myocardium [Abstract]. *Fed Proc* 1985;44:823.

18. Lowe JE, Reimer KA, Jennings RB. Evidence that ischemic cell death begins in the subendocardium independent of variations in collateral flow or wall tension. *Circulation* 1983;68:190–202.

EDITORIAL
Is Nuclear Medicine Viable and Can It Measure Viability?

Like the other imaging modalities, nuclear medicine is moving along the road towards being a discipline of prognosis rather than diagnosis. One way that this will be accomplished is by the development of new radiophar-maceuticals that will take us further from the morphologic imaging realm which the other imaging modalities do so well, into the area of functional im-aging based upon the underlying bio-chemistry. Although PET radiophar-maceuticals have dominated the field of functional imaging based upon bio-chemistry in the past, new, single-photon based radiopharmaceuticals are being developed which challenge or even exceed PET's dominant posi-tion. One such example is the devel-opment and use of radiolabeled soma-tostatin analogues not just to identify tumor tissue, but more importantly, to predict the sensitivity of the tumor tis-sue to therapy using somatostatin it-self (*1*). This situation, where a thera-peutic drug is converted into a diagnostic drug, is unusual and in this case results in a highly specialized ap-plication. A more general desire is to develop a radiopharmaceutical that is able to indicate the (biochemical) functioning of a piece of tissue such as the oxygen sensing iodovinylmi-sonidazole (IVM) described by Martin et al. in this issue (*2*).

The functioning of a piece of tissue

is governed by the laws of supply and demand. Within limits, output can in-crease so long as the demands are met by an increase in supply of the neces-sary nutrients. For short periods of time, demand can exceed supply at the cost of producing a nutrient debt. As the supply is reduced, the maxi-mum output is restricted and systems must be downregulated to maintain vi-ability. Below some set point, which can be changed, this results in a ces-sation of output from the tissue. Fur-ther reductions in supply lead ulti-mately to cell death. When supply and demand are coupled and the tissue is stable, we can use perfusion, a crude measurement of supply, to assess the status of the tissue on a regional basis. In the case of the brain, we interpret the demand as that required by the expected normal neurological func-tioning. In the case of the myocar-dium, we interpret the demand as that required by the contractile function of the heart. When the normal function-ing of the tissue is changed such that we cannot interpret what the demand is, perfusion becomes of less value and we need instead a measure of the potential for recovery (viability) of the tissue. Such is the case in ischemic myocardium or presentations of hiber-nating or stunned tissue (*3*).

The energy state of the cell is a measure of viability: This is, however, hard to obtain in a noninvasive man-ner, partly because of the variety of pathways the cell can use to produce its energy. A number of radio-pharmaceuticals have been proposed

as viability markers which measure some aspect of the energy state of the myocardium (FDG, thallous ion, palmitate, acetate), but all have their deficiencies (*4*). Our understanding of the information content of a myocar-dial FDG image is, for instance, still far from complete (*5,6*) and even the conditions for obtaining one are still being refined (*7,8*). The assessment of viability is not, of course, only de-sirable for the myocardium but is rel-evant to patient management for all situations where ischemia is a compo-nent of the disease. This includes stroke, where delayed presentation and progression of the insult combine to make assessment of intervention options difficult, and oncology, where treatment is reliant on differences in metabolic rates and (undesirable) via-bility. Tissue oxygenation is an acces-sible common denominator to the cel-lular energy equation (*9*) and so a variety of methods for measuring tis-sue oxygen levels have been devel-oped (*10*). The potential for using ra-diopharmaceuticals based upon the radiosensitizer, misonidazole, to de-pict hypoxic tissue in vivo noninva-sively was recognized by Chapman in 1979 (*11*). The mechanism that causes trapping in hypoxic tissue relies on the competition between enzymatic re-duction and ensuing reoxidation by molecular oxygen. Thus, nitroimida-zoles are not retained in well oxygen-ated tissue because of efficient reoxi-dation of the species that lead to trapping. Nor are they retained in se-verely damaged tissue in which the